Short Communication

Development of an Electrochemical Sensor for Chloride ion Detection Using Ion-Sensitive Field-Effect Transistor Array

Xinxin Yuan[1,2], Xuelian Zhang[1], Yizheng Huang[1,3], Junyao Jie[1,3], Qingquan Wei[1],
Manqing Tan[1,3] and Yude Yu[1,2,3,]*

[1] State Key Laboratory of Integrated Optoelectronics, Institute of Semiconductors, Chinese Academy of Sciences, P.O. Box 912, Beijing 100083, PR China
[2] School of Electronics, Electrical and Communication Engineering, University of Chinese Academy of Sciences, Beijing 100049, China
[3] College of Materials Science and Opto-Electronic Technology, University of Chinese Academy of Sciences, Beijing 100049, China
[*]E-mail: yudeyu@semi.ac.cn

In this study, we designed a p-channel 32×48 ion-sensitive field-effect transistor (ISFET) array sensor with a modified membrane to detect chloride ion concentration. The proposed sensor includes three parts, i.e., an ISFET array, readout interfacing circuits, and row/column selection circuits. The unmodified ISFET array sensor was immersed in solutions with pH ranging from 2.88 to 10.40, and the sensing characteristics were evaluated. A high sensing average sensitivity(55.6 mV/pH) and linearity (0.945) were demonstrated. Then, a chloride ion-sensing membrane was dropped on the floating gate of the ISFET sensor. To evaluate the sensing characteristics of the chloride ion sensor, the sensor was immersed in different concentrations of NaCl solutions ranging from 10^{-5} M to 10^{-1} M. The average sensitivity and linearity of the chloride ion sensor were 51.8 mV/pCl and 0.990, respectively.

1. INTRODUCTION

Chloride ion (Cl⁻) is the most abundant anion in living organisms and therefore, it is crucial in several fields. In clinical analysis, intra- and extra-cellular chloride ions participate in various biological functions through transmembrane transport and ion channels [1,2]. The concentration of chloride ions in human body fluids, such as sweat, plays a crucial role in determining the biological features of certain serious diseases, such as cystic fibrosis [3]. During environmental monitoring processes, several studies have reported that chloride ions are one of the main reasons for the corrosion of steel in reinforced

concrete structures. This implies that the detection of chloride ion concentration in concrete covers and steel reinforcements is necessary to assess the corrosion-related risks [4]. In daily life, the concentration of chloride ions in food and drinking water is an indicator of their quality, with large chloride ion concentrations implying that the food is unhealthy [5].

Previously reported studies have proposed several methods for the detection of chloride ions, such as ion chromatographic colorimetry [6], the Mohr method [7], inductively coupled plasma optical emission spectrometry (ICP-OES) [8], and fluorometry [9]. Most of these methods require the use of bulky and expensive measuring instruments, which limit their applications; furthermore, the time consumption, complexity of operations, and high detecting costs limit their applications of these methods. Therefore, it is crucial to develop a rapid, sensitive, selective, and portable electrochemical method for the determination of chloride ions. Contemporary analysis methods for chloride ions via point-of-care testing (POCT) use electrochemical detection, which is implemented via portable and highly sensitive devices; these methods are being increasingly used by researchers [10,11]. For example, Bin et al. [12] fabricated a silver nanoparticles-modified glassy carbon electrode to measure the chloride ion concentration. However, conventional chloride ion-selective electrodes (ISEs) cannot be used for certain applications because the AgCl of ISEs may pollute the detecting proteins [13]. The ion-sensitive field-effect transistor (ISFET), developed by Bergveld [14] in 1970, has been widely used for electrochemical sensing of the ion concentration in a solution [15]. The structure of ISFET was proposed based on the structure of metal-oxide-semiconductor field-effect transistor (MOSFET), which has attracted considerable attention for biomedical, biochemical and industrial applications. The surface potential of ISFET device at the interface between the ion-sensing membrane and electrolyte depends on the specific ion concentration in the electrolyte, which results in a change in the flat-band voltage [16]. ISFET has been reported to detect pH values [17–19], and concentration of other ions [20,21]. Generally, ISFET is used in biochemincal, biomedical [22–28], and environmental monitoring fields [29].

In this study, we developed a chloride ion sensing membrane modified p-channel Si_3N_4 ISFET array sensor with integrated readout interfacing circuits, ISFET array, and row/column selection circuits to obtain and detect the concentration of chloride ions, with a sensor power consumption of 1.8 V×7 mA. The detection range of the developed sensor was satisfactorily linear, and it was successfully applied in the analysis of chloride ions in NaCl. In addition, excellent analytical performance of the chloride ion sensor was achieved, including sensitivity and stability, which is highly significant for the application of the sensor in electrochemical sensing.

2. EXPERIMENTAL

2.1. Reagents and instruments

Bis(2-ethylhexyl) sebacate (DOS), sodium chloride (NaCl), polyvinyl chloride (PVC), and tetrahydrofuran (THF) were purchased from Aladdin Reagent Company (Shanghai, China). Tridodecylmethylammonium chloride (TDDMACl) and chloride ionophore III (ETH 9033; 3,6-

Didodecyloxy-4,5-dimethyl-o-phenylene-bis(mercury chloride)) were purchased from Sigma-Alorich Co. Ltd. (St. Louis, MO, USA). Hydrochloric acid (HCl) and sodium hydroxide (NaOH) were purchased from Beijing Chemical Works (Beijing, China).

A data acquisition card (ART USB2884) was used to collect the response voltage, a field-programmable gate array (FPGA, Xilinx Spartan6) was used to provide the clock pulse signal, a power source (Keithley 2450) was used to provide the specific voltage, and a computer was used to control the measuring system.

2.2. Fabrication of the ISFET array sensor

We designed a 32×48 ISFET array sensor comprising an ISFET array, readout interfacing circuits (ROIC), and row/column selection circuits, as shown in Fig. 1. The sensor was fabricated using a 0.18 μm standard CMOS process from the Global Foundries Company. The entire layout of the chip occupied an area of 2540 μm × 2950 μm, and the area of the sensing window was 1920 μm × 2880 μm.

The ROIC circuit, as shown in Fig. 2, was applied to obtain the output voltage that varied with the chloride ion concentration of the sample, and the change was detected by the chloride ion-sensing membrane-modified ISFET array.
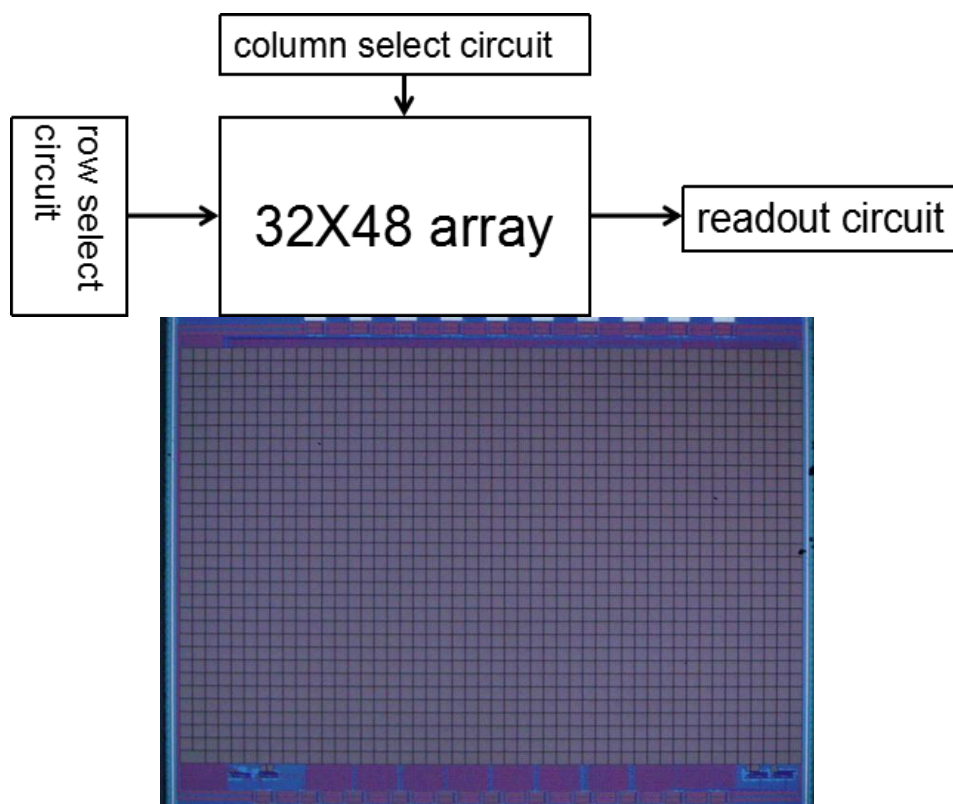

Figure 1. Block diagram and microscopic image of ISFET array sensor.

The current source and voltage followers were used to provide ROIC biasing in this circuit. The two operational amplifiers (op-amps, A_1 and A_2) functioning as voltage followers with unity gain were

used to keep the voltage biasing constant. Thereafter, the current source (I_{D2}) along with the resistor (R_V) maintained a constant drain-source voltage (V_{DS}) of the ISFET because the current confined to the operational amplifier A_2 was negligible. The gate-source voltage (V_{GS}) changed when the floating gate potential was altered by varying the ion concentration in the electrolyte. Finally, the output voltage was reflected in V_S because V_G was fixed, and the drain–source voltage was constant [30]. The row/column selection circuit based on D-type flip-flops provided row/column selection signals to select a specific pixel in the ISFET array conducting with the ROIC circuit, as shown in Fig. 3. The clock pulse signal needed for the circuit was provided using a FPGA.
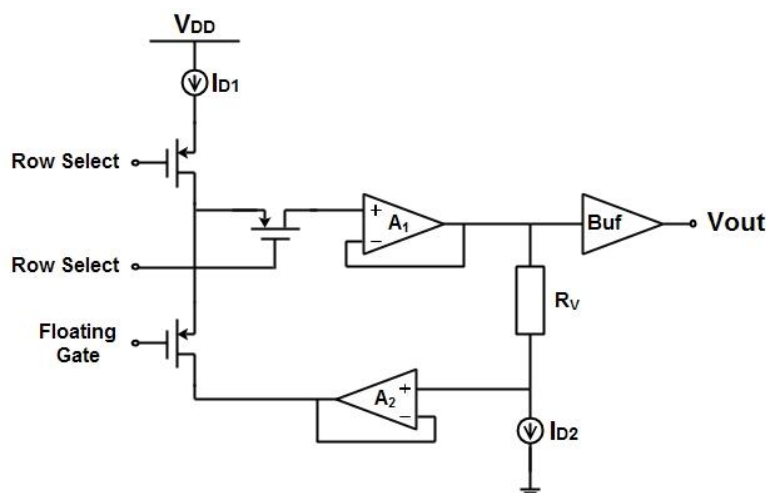
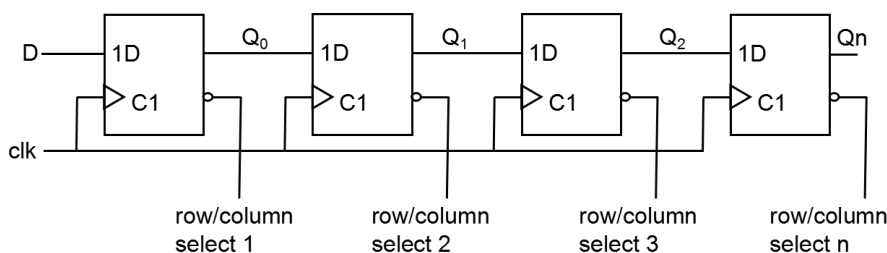

Figure 2. Schematic of the ROIC circuit.

Figure 3. Schematic of D-type flip-flops.

2.3. Fabrication of the chloride ion sensor

The chloride ion-sensing membrane comprised PVC/DOS/ETH9033/TDDMACl in the ratio 33:66:2:10 (wt%) [31], which is the optimum chemical composition. The chloride ion-sensing mixture was placed in an ultrasonic cleaner for 30 minutes to properly mix the ingredients. Then, 2 µL of the homogeneous mixture was dropped on the floating gate of the chip. To ensure optimum performance of the chloride ion sensor, such as stability and sensitivity, the chloride ion sensor was placed on a Clean Bench for 24 hours at 25 °C until the mixture solidified to form the ion-sensing membrane, which was then fully immobilized on the chip. This process is essential for the fabrication of a chloride ion sensor because the application of the wet ion-sensing membrane increases the standard error in the response

voltage. Finally, the chloride ion sensor fabrication was completed as per the method described by Chou et al[13]. To add the testing solution to the sensor, it is necessary to electrically connect the contact pads of the ISFET array chip with the conducting lines on the PCB substrate by wire bonding. An optical adhesive/underfill was used to cover the bonding wires for avoiding short circuits, and then a plastic case of approximately 2mL in volume, wherein the solution to be assayed was placed, was positioned on the top of the sensor's sensitive area. The encapsulated chloride ion sensor is shown in Fig. 4.
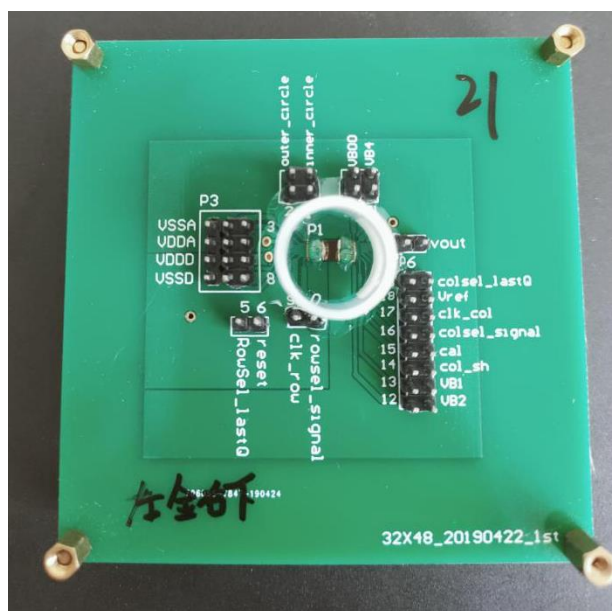

Figure 4. Photograph of the encapsulated chloride ion sensor

2.4. Measuring system

The measuring system comprised a computer, data acquisition card (DAQ), power supply, FPGA, and chloride ion sensor. The FPGA was used to construct a 5-channel clock pulse signal (250 k Hz), and was connected with a DAQ and four row/column selection circuits on the sensor. The operating software of the measuring system was designed based on an Art control software, which controlled the chloride ion sensor according to a predetermined method. Ag/AgCl electrode was connected to the electrolyte solution as a reference electrode to maintain the stability of electrolyte potential. The measurement was conducted using the voltage–time measuring system for detecting the concentration of chloride ions in different NaCl solutions. The measuring system is shown in Fig. 5. The measuring system was designed to detect the sensitivity and drift potentials, and was controlled by a computer. The response voltages were collected using the DAQ, and were then transmitted to the computer, wherein they were analyzed using MATLAB software.
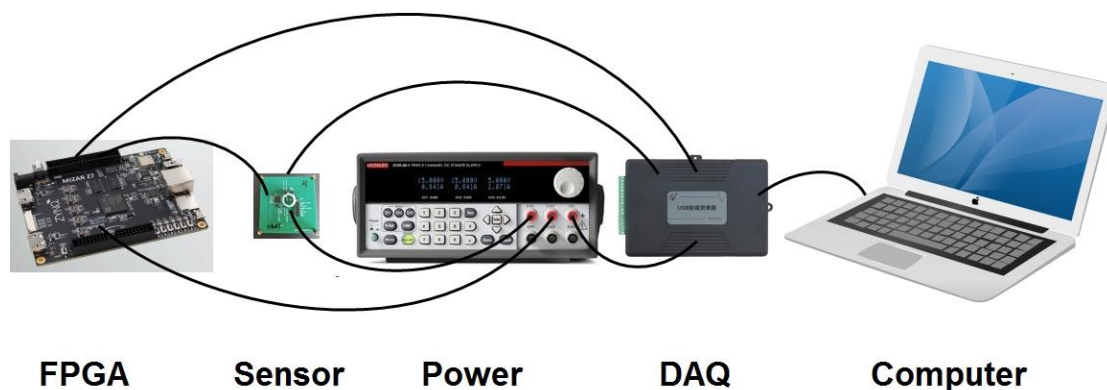
Figure 5. Measuring system of the chloride ion sensor.

3. RESULTS AND DISCUSSION

3.1. Measurement results of the ISFET array sensor

Compared with the operational theory of the traditional MOSFET, the ISFET was developed using its floating gate characteristic curves to explore the relationship between the threshold voltage and concentration of the sample ion. From the ROIC circuit mentioned in section 2.2, we know that the ISFET device operates in a linear detection range, with constant drain-source voltage (V_{DS}). These mechanisms changes the V_{GS} value as the threshold voltage(V^*_{TH}) is varied, and these variations are directly proportional to the variation in the pH value based on the following equation[32]:

$$I_{DS} = \mu_n C_{ox} \frac{W}{L}[(V_{GS} - V^*_{TH})V_{DS} - \frac{1}{2}V^2_{DS}], \qquad (1)$$

where $V^*_{TH} = V_{TH} + \zeta$, and ζ is the interface potential between the ion-sensing membrane and the electrolyte solution.

In the ISFET array, the two outermost rings of pixels were connected with an input voltage (similar to that in a MOSFET) to test the electronic signal of the chip, and to ensure efficient chip operation. After the contact pads of the sensor chip were electrically connected to the conducting lines on the PCB substrate through wire bonding, an electrical test was conducted. We tested the response voltages with the change in the gate voltages of the two outermost rings of pixels, and the gate voltage varied from 0 to 200 mV. Based on the experimental results, as shown in Fig. 6(a), the response voltages of the two outermost rings of pixels was approximately 1.0 V and the voltage of the floating gate pixels was approximately 1.32 V, which proves that the chip was in good electrical working condition. There were small differences in the response voltages of the two outermost ring pixels; we suspected that this may be caused by the unreasonable wire layout in the chip.

For the electrolyte solutions, a 0.01 mol/L sodium chloride (NaCl) solution was prepared to prevent the interference of other ions during detection, and the pH value was regulated by adding HCl or NaOH solution. Electrolyte solutions were selected with pH values of 2.88, 3.70, 4.27, 5.51, 7.01,7.70, 8.10, and 10.40 as samples. Then the array was scanned to obtain the corresponding matrices; one of the results is shown in Fig. 6(b). The response voltages of some pixels in the floating gate remained high.

This is due to the covering of the floating gate with optical adhesive/underfill, which was applied to protect the bonding wires; however, this sensor packaging method can result in a loss of sensing area.

Then, some pixels were then selected for plotting the response voltage–pH curves, which were used to express the sensitivity of the sensor. The least-square method was applied to obtain linear curve fittings, and the slope was considered to indicate sensitivity. An average sensitivity of 16.0 mV/pH was obtained, which was much lower than the theoretical value. This could be caused by the oxidation of the sensitive Si_3N_4 layer at the top of the floating gate. Thereafter, a buffered oxide etch (BOE) solution was used to treat the top layer of the floating gate for several minutes, and the sensitivity was determined with average sensitivity value of 55.6 mV/pH. A random pixel was tested, as shown in Fig. 7, and a sensitivity and linearity of 55.3 mV/pH and 0.944 were obtained, respectively.
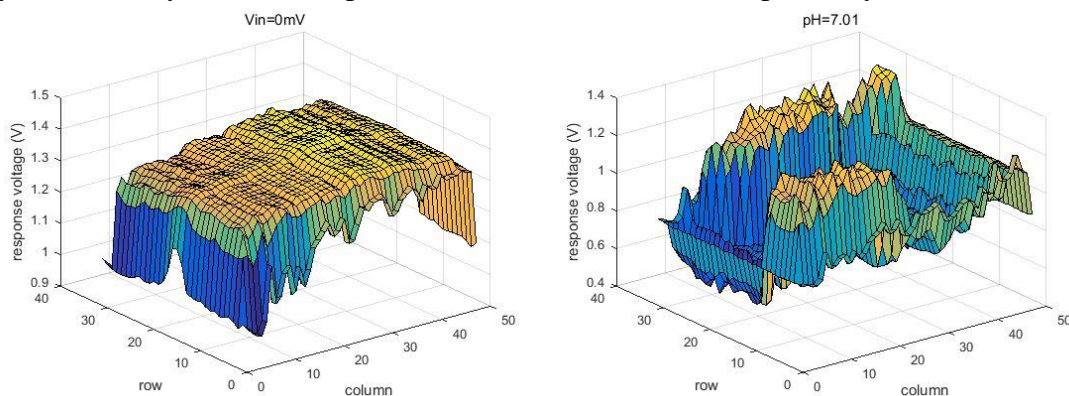

Figure 6. (a) Response voltages of the sensor when the input voltage of the two outermost rings of pixels was 0 mV; (b) response voltages of the sensor with the pH of the electrolyte solution was 7.01.
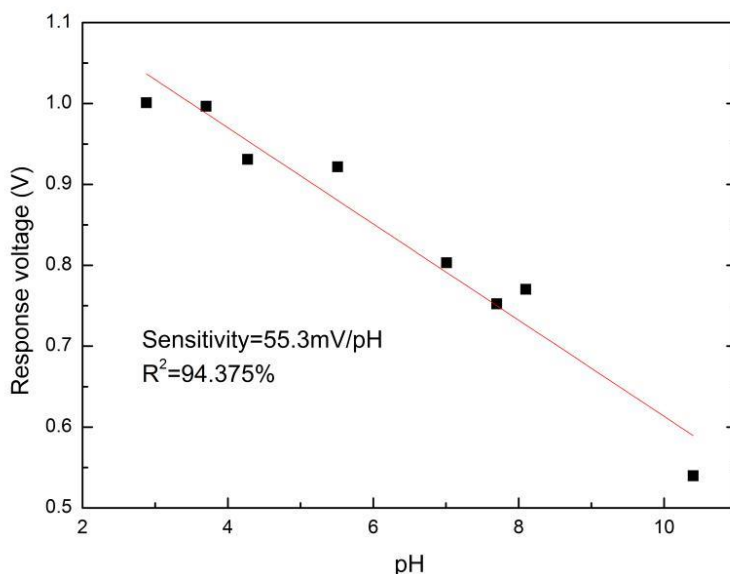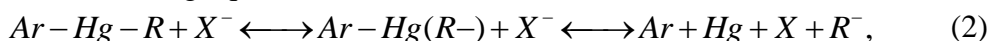

Figure 7. Curves of response voltage versus pH for the ISFET array sensor.

3.2. Measurement results of the chloride ion sensor

ETH9033 was found to possess excellent selectivity for Cl⁻, where the sensing mechanism is based on the following equation:

$$Ar - Hg - R + X^- \longleftrightarrow Ar - Hg(R-) + X^- \longleftrightarrow Ar + Hg + X + R^-, \qquad (2)$$

where Ar–Hg–R is the mercury organic compound and X is the chloride ion. The best ratio of the chloride ion-sensing membrane was PVC 33%, ETH9033 2%, DOS 66%, and TDDMACl 10%, which showed great sensitivity and linearity [31]. Moreover, the relationship between the response voltage and chloride ion concentration can be determined using the following equation [13]:

$$E = E_0 - 2.303 \frac{RT}{F} \log \alpha = E_0 - 0.05916 pCl, \quad (3)$$

where E is the electromotive force (EMF), E_0 is the initial voltage, α is the activity of the ion, R is the gas constant, and F is the Faraday coefficient. The chloride ions in the electrolytes were attached to the sensing membrane of the sensor to further produce the EMF. The response voltages were then transmitted to the measuring system. The software was used to measure the response voltages for different chloride ion concentrations. Equation (3) shows that the response voltage varies linearly with the chloride ion concentration.

For NaCl solutions with concentration ranging of 10^{-1} M to 10^{-5} M, the average detection sensitivity of the ISFET array chloride ion sensor was 51.8 mV/pCl and the linearity was 0.990 . The experiment results obtained for the same pixel, as described in Section 3.1, are shown in Fig. 8(a). Compared with the findings of related studies, as listed in Table 1, we observed that the chip in this study has better sensitivity and linearity. The experimental results prove that the chloride ion sensor exhibited excellent sensing performance.

An important characteristic of the sensor is the average drift voltage. Fig. 8(b) shows the response voltages within 800 min of successive testing of the proposed chloride ion sensor immersed in a 10^{-2} M NaCl solution. The response voltages of the chloride ion sensor gradually stabilized after 200 min of successive testing, and the average drift voltage of the sensor was approximately 5.0 mV/h.
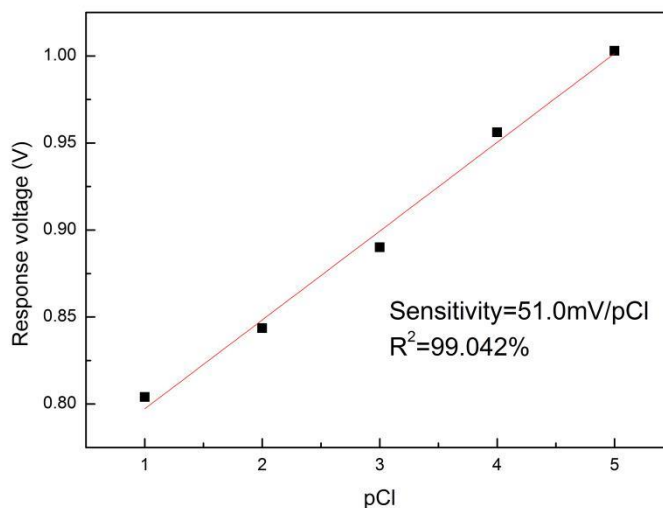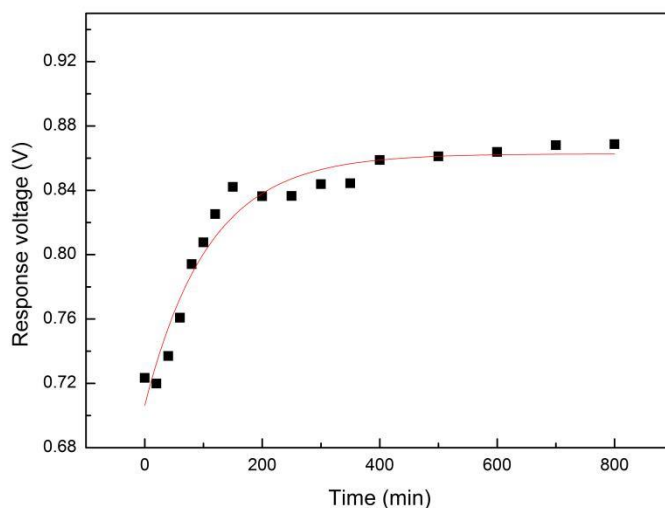
Figure 8. (a) Curves of the response voltage versus concentration for the chloride ion sensor for NaCl solutions with concentrations from 10^{-1} M to 10^{-5} M; (b) curve of the response voltage versus time of the chloride ion sensor in a 10^{-2} M NaCl solution.

Table 1. Comparison of the average sensitivity and linearity between chloride ion sensors from our study and other studies.

Ref	Error! Reference source not found.	Error! Reference source not found.	Error! Reference source not found.	Error! Reference source not found.	Error! Reference source not found.	Our work
Type of electrodes	ISE	ISE	EGFET	ISE	ISFET	ISFET
Sensing materials	RuO_2	IGZO/Al modified by graphene oxide	Cr/Au	RuO_2	Si_3N_4	Si_3N_4
Sensitivity (mV/pCl)	44.445	60.536	42	22.42−24.14	42−43	51.8
linearity	0.971	0.973	0.988	0.841−0.91		0.990

Stability is another important factor in the application of the proposed electrochemical sensor. The modified sensor was stored for 3 weeks at room temperature, and the sensitivity of the sensor to the chloride ion solution was almost the same as that of the initially obtained analytical result. After 7 months, the sensitivity was 40.0 mV/pCl and the linearity was 0.994, which is close to 80% of its initial sensitivity value. The above results suggest that the proposed sensor is highly stable.

4. CONCLUSIONS

Herein, we developed a small sensor to meet specific requirements for detecting chloride ion concentrations. The sensor was made up of three modules, i.e., an ISFET array sensor, chloride ion-sensing membrane, and measuring system. The ISFET array sensor consisted of an ISFET array, row/column selection circuits, and readout interfacing circuits, which provided fast and stable detection of the ion concentration. The chloride ion-sensing membrane consisted of an organic solvent in a solute

that was dropped on the sensing window, and the membrane was prepared through solvent volatilization. The measuring system was controlled by a computer, and the response voltages were captured and displayed on the computer. We integrated all circuits into the sensor chip, which greatly increased integrity and reduced the sensor area, therefore the chloride ion sensor has the advantages of high integration, low power consumption, small volume, cost-efficiency, high sensitivity, better selectivity and stability , and it can be produced on a large scale.

The chloride ion sensor was designed to measure the concentration of NaCl solutions. We obtained an average pH sensitivity of 55.6 mV/pH without a chloride ion-sensing membrane. After the pH test, the chloride ion-sensing membrane solution was dropped on the sensing window of the sensor to detect the chloride ion concentration. The average sensitivity and linearity were 51.8 mV/pCl and 0.990 within the NaCl concentration range of 10^{-1} M to 10^{-5} M, respectively. After 7 months, the sensitivity was 40.0 mV/pCl and the linearity was 0.994. The results showed that the chloride ion sensor had great sensing characteristics and stability.

References

1. V. Faundez, H. C. Hartzell, *Sci. STKE2004*, re8 (2004).
2. J. C. Chen, Y. F. Lo, Y. W. Lin, S. H. Lin, C. L. Huang and C. J. Cheng, *Proc. Natl. Acad. Sci.*, 116(10) (2019) 4502.
3. V. A. LeGrys, T. C. Moon, J. Laux J, F. Accurso and S.A. Martiniano, *J. Cyst. Fibros.*, 18(2) (2019) 190.
4. U. Angst, B. Elsener, C. K. Larsen and Ø. Vennesland, *J. Appl. Electrochem.*, 40 (2010) 561.
5. C. Lopez-Moreno, I. Viera Perez, *A.M. Food Chem.*, 194 (2016) 687.
6. J. S. F. Pereira, L. O. Diehl, F. A. Duarte, M. F. P. Santos, R. C. L. Guimaraes, V. L. Dressler, and E. M. M. Flores, *J. Chromatogr. A*, 1213 (2008) 249.
7. R. T. Sheen, H. L. Kahler, W. H, L. D. Betz and Philadelphia. Pa, *Ind. Eng. Chem., Anal. Ed*. 10 (1938) 628.
8. J. Naozuka, M. A. Mesquita Silva da Veiga, P. V. Oliveira and E. D. Oliveira, *J. Anal. Atomic. Spectrom.*, 18 (2003) 917.
9. M. Tsukimoto, H. Harada, A. Ikari and K. Takagi, *J. Biol. Chem.*, 280 (2005) 2653.
10. S. C. Tseng, T. Y. Wu, J. C. Chou, Y. H. Liao, C. H. Lai, J. S. Chen, S. J. Yan, M. S. Huang, T. W. Tseng and Y. H. Nien, *Mater. Res. Bull.*, 101 (2018) 155.
11. S. Cinti, D. Talarico, G. Palleschi, D. Moscone and F. Arduini, *Anal. Chim. Acta*, 919 (2016) 78.
12. Q. Bin, M. Wang and L. Wang, *Nanotechnology*, 31 (2020) 125601.
13. J. C. Chou, T. W. Tseng, and Y. H, Liao, C. H. Lai, S. J. Yan, Y. X. Wu, C. Y. Wu and S. H. Lin, *IEEE Sens. J.*, 19 (2019) 3217.
14. P. Bergveld, *IEEE Trans. Biomed. Eng., BME*-17 (1970) 70.
15. S. Nakata, T. Arie, S. Akita and K. Takei, *ACS Sens.*, 2 (2017) 443.
16. L. Bousse, S. Mostarshed, B. van der Schoot and N. F. de Rooij, *Sens. Actuators B Chem.*, 17

(1994) 157.

17. H. S. Wong, M. H. White, International Electron Devices Meeting. Technical Digest, IEEE, (1988) 658.
18. L. Wang, L. Li, T. Zhang, X. Liu and J-P. Ao, *Appl. Surf. Sci*., 427 (2018) 1199.
19. C. H. Hsieh, I. Y. Huang and C. Y. Wu, *Sensors,* (2010) 358.
20. Y. T. Chen, I. Sarangadharan, R. Sukesan, C. Y. Hseih, G. Y. Lee, J. I. Chyi and Y. L. Wang, *Sci. Rep.*, 8 (2018) 1.
21. C. Bao, M. Kaur and W. S. Kim, *Sens. Actuators B Chem*., 285 (2019) 186.
22. S. Ma, Y. K. Lee, A. Zhang and X. Li, *Sens. Actuators B Chem*., 264 (2018) 344.
23. R. Ahmad, N. Tripathy, J. H. Park and Y. B. Hahn, *Chem. Commun*., 51 (2015) 11968.
24. N. Ruecha, J. Lee, H. Chae, H. Cheong, V. Soum, P. Preechakasedkit, O. Chailapakul, G. Tanev, J. Madsen, N. Rodthongkum, O. S. Kwon and K. Shin, *Adv. Mater. Technol*., 2 (2017) 1600267.
25. S. Machida, S. Hideto, *Y. J. Appl. Phys*., 47 (2018) 04FM03.
26. N. Formisano, N. Bhalla, M. Heeran, J. Reyes Martinez, A. Sarkar, M. Laabei, P. Jolly, C. R. Bowen, J. T. Taylor, S. Flitsch and P. Estrela, *Biosens. Bioelectron*., 85 (2016) 103.
27. P. Firek, M. Cichomski, M. Waskiewicz, I. Piwonski and A. Kisielewska, *Circuit World*, 44 (2018).
28. M. W. Shinwari, M. J. Deen and D. Landheer, *Microelectron. Reliab*., 47 (2007) 2025.
29. C. Jimenez-Jorquera, J. Orozco and A. Baldi. *Sensors*, 10 (2010) 61.
30. N. L. M. A. Samah, K. Y. Lee, S. A. Sulaiman and R. Jarmin, *Int. Conf. IEEE Eng. Med. Biol. Soc. IEEE,* (2017), 869.
31. J. C. Chou, G. C. Ye, D. G. Wu and C. C. Chen, *Solid-state Electron*., 77 (2012) 87.
32. W. Y. Chung, K. C. Chang, D. Y. Hong, C. Cheng, F. Cruz, T. S. Liu, C. H. Yang, D. G. Pijanowska, M. Dawgul, W. Torbicz, P. B. Grabiec and B. Jarosewicz, 17th Biennial University / Government / Industry Micro/Nano Symposium, (2008) 44.